Antranik A. Siranosian[1]
e-mail: aasiranosian@gmail.com

Miroslav Krstic

Andrey Smyshlyaev

Department of Mechanical and
Aerospace Engineering,
University of California, San Diego,
La Jolla, CA 92093

Matt Bement
Los Alamos National Laboratory,
Los Alamos, NM 87545

Gain Scheduling-Inspired Boundary Control for Nonlinear Partial Differential Equations

We present a control design method for nonlinear partial differential equations (PDEs) based on a combination of gain scheduling and backstepping theory for linear PDEs. A benchmark first-order hyperbolic system with an in-domain nonlinearity is considered first. For this system a nonlinear feedback law, based on gain scheduling, is derived explicitly, and a proof of local exponential stability, with an estimate of the region of attraction, is presented for the closed-loop system. Control designs (without proofs) are then presented for a string PDE and a shear beam PDE, both with Kelvin–Voigt (KV) damping and free-end nonlinearities of a potentially destabilizing kind. String and beam simulation results illustrate the merits of the gain scheduling approach over the linearization based design. [DOI: 10.1115/1.4004065]

1 Introduction

The stabilization of nonlinear partial differential equations (PDEs) is an important area in control design motivated by real-world applications in the areas of thermal, reaction, fluid, structural, and plasma systems. Several control design methods for PDEs have been reported in the literature. We discuss only those that are relatively broadly applicable rather than being for a single specific PDE. Finite-dimensional backstepping methods were used for the design of stabilizing boundary controllers for spatially discretized parabolic PDEs in Refs. [1–3]. Statistical-based model reduction techniques were presented in Refs. [4–6]. Nonlinear model reduction and input–output feedback linearization for quasilinear first-order hyperbolic and parabolic systems were presented in Ref. [7]. Passivity based exponentially stabilizing control design and a flatness based approach for trajectory generation for flexible structures were presented in Ref. [8]. Feedforward and feedback controllers based on formal power series parameterization and summation methods for stabilization and tracking for nonlinear PDEs were presented in Ref. [9]. A gain scheduling approach for nonlinear PDEs in Ref. [10] used a linearization based approach, where controllers were designed for the finite-dimensional approximation of the system linearized about a family of operating points. An approach for full state feedback linearization for a broad class of nonlinear parabolic partial integro-differential equations (PIDEs) was presented in Refs. [11,12], where the nonlinear feedback operators are constructed using Volterra series in the spatial variable.

This paper presents a gain scheduling inspired control design for nonlinear PDEs based on the backstepping approach for linear PDEs. Gain scheduling [13–22] is a technique that replaces a fully nonlinear control design (such as, for example, backstepping or forwarding, which yield global stability) with the design of a family of linear controllers that are implemented according to a scheduling signal. It requires linearizing the plant about a family of operating points (for example, see Refs. [18,23,24]) or the formulation of the model in a quasi-linear parameter varying (LPV) form (for example, see Refs. [18,21]), such that linear control

tools can be applied. PDE backstepping [25] is an approach for the design of boundary controllers for infinite dimensional PDE models without discretization or model reduction. As a form of model reference control for infinite dimensional systems, state transformations relating a closed-loop system to a target system are used to design stabilizing controllers.

Here the design of a stabilizing controller begins by writing the PDE model in a form to which gain scheduling techniques apply. Once in the appropriate form, gain scheduled PDE backstepping transformations—similar to standard PDE backstepping transformations in structure, but employing state-dependent transformation gains—are used to relate the nonlinear PDE model to a target system. Unlike typical gain scheduled controllers, where either the controller or its parameters are scheduled, the resulting controllers in this work are applied as nonlinear controllers (linear controllers with "continuously scheduled" state-dependent parameters). While not as powerful as the exactly linearizing nonlinear PDE backstepping boundary controllers in Refs. [11,12], gain scheduling controllers are a simpler and much more manageable design alternative for the challenging problem of nonlinear PDE control, with performance advantages over linearization based designs. Note that this work does not pursue the proof of existence and uniqueness of solutions for the PDEs considered, and the control designs are done assuming unique solutions exist.

We first present an explicit gain scheduling based control design for a benchmark first-order hyperbolic PDE with a boundary-value-dependent in-domain nonlinearity, which is an extension of the result in Ref. [26]. For this benchmark system we present a detailed analysis of local exponential stability, with an estimate of the region of attraction. Even for this relatively simple nonlinear PDE system, the analysis is quite complex and highlights the issues that one would face in performing a stability analysis for more complex nonlinear PDEs with gain scheduling controllers. These issues include the construction of Lyapunov functionals using nonlinear backstepping transformations, the bounding of nonlinear terms left uncompensated in the gain scheduling approach, and perhaps most importantly, the choice of system norms and the derivation of stability estimates and regions of attraction in high enough Sobolev norms to capture the effect of nonlinear perturbations in the stability analysis.

We then turn our attention to some relevant basic mechanical PDE systems—the string and shear beam PDEs with Kelvin–Voigt damping and boundary-displacement-dependent free-end

---

[1]Corresponding author.
Contributed by the Dynamic Systems Division of ASME for publication in the Journal of Dynamic Systems, Measurement, and Control. Manuscript received December 12, 2008; final manuscript received February 26, 2011; published online August 1, 2011. Assoc. Michael A. Demetriou.

nonlinearities. These designs are the extensions of results for the string [27–30] and shear beam [29–32]. The merits of these designs are highlighted by simulation. Motivation for these systems comes from shake table control and from atomic force microscopy. In a particular shake table control problem, the table provides boundary actuation to a structure in order to impart a desired reference trajectory at some point near its free-end, which possibly exhibits nonlinear behavior. In atomic force microscopy, the base of a cantilevered beam is actuated to stabilize a probe at its free-end, which interacts nonlinearly with the sample surface.

This work introduces a *completely new framework* for PDE backstepping designs, though the designs do employ past results for linear PDEs. This new approach allows for the design of *explicit* nonlinear controllers for PDEs, rather than controllers given in the form of a nonlinear Volterra series, as in Refs. [11, 12]. Also, the analysis techniques introduced for the nonlinear hyperbolic PDE are far beyond those previously employed in backstepping designs for linear PDEs.

The paper is organized as follows. Section 2 presents the gain scheduling based control design for a benchmark first-order hyperbolic PDE with boundary-value-dependent in-domain nonlinearity, and the proof of stability for the resulting closed-loop system. Sections 3 and 4 present the control design and simulation results for a string with Kelvin–Voigt damping and boundary-displacement-dependent free-end nonlinearity. Section 5 presents the control design for the shear beam with Kelvin–Voigt damping and boundary-displacement-dependent free-end nonlinearity. Section 6 presents simulation results for the Timoshenko beam with Kelvin–Voigt damping and boundary-displacement-dependent free-end nonlinearity, based on the shear beam designs of Sec. 5.

2 Gain Scheduling Design for a Benchmark First-Order Hyperbolic PDE

Consider the first-order hyperbolic PDE with a boundary-value-dependent in-domain nonlinearity

$$u_t(x,t) = u_x(x,t) + g(u(0,t))e^{b(u(0,t))x}u(0,t) \tag{1}$$

where $u(x,t)$ is the state of the system on the domain $0 \le x \le 1$ at time $0 \le t < \infty$, with initial condition $u_0(x) = u(x,0)$. Control is applied at $x = 1$ through the boundary condition $u(1,t)$. The functions $b(\cdot)$ and $g(\cdot)$ are arbitrary continuously differentiable functions. The nonlinearity $g(u(0,t))e^{b(u(0,t))x}u(0,t)$—which corresponds to an effect called "recirculation" in chemical tubular reactors—destabilizes the origin of the open-loop system (1), $u(1,t) = 0$, therefore some form of control is needed to stabilize the equilibrium $u \equiv 0$.

Though the gain scheduling design can be developed (and proved) for a much broader class of PDEs (not only first-order hyperbolic but also parabolic and second-order hyperbolic), and where nonlinearities include dependence on the full state $u(x,t)$, rather than on $u(0,t)$ only, Eq. (1) is used as a benchmark problem because all the steps of the analysis can be completed by explicit calculations.

The following steps are taken for the gain scheduling based PDE backstepping design. First, the nonlinearity is written in the quasilinear parameter varying form $\bar{f}(\cdot)u(\cdot)$. Following gain scheduling techniques $\bar{f}(\cdot)$ is considered to be a constant $\bar{f}$, then PDE backstepping techniques are used to find transformations relating the plant to a target system. Having found the transformations, $\bar{f}$ is replaced by $\bar{f}(\cdot)$, and a gain scheduling based nonlinear controller is found using PDE backstepping techniques. When work has already been done for a system with constant $\bar{f}$, i.e., a linear force, then $\bar{f}(\cdot)$ can simply be substituted for $\bar{f}$ in those results.

For the current problem, the nonlinearity $g(u(0,t))e^{b(u(0,t))x}u(0,t)$ is already in the LPV form, with $\bar{f}(\cdot) = g(\cdot)e^{b(\cdot)x}$. Moti-

vated by Ref. [26, example 2.1] where b and g are constant, this work introduces the backstepping transformations

$$w(x,t) = u(x,t) - \int_0^x k(x,y,u(0,t))u(y,t)\,dy \tag{2}$$

$$u(x,t) = w(x,t) + \int_0^x l(x,y,w(0,t))w(y,t)\,dy \tag{3}$$

where in the present problem with $b(u(0,t))$ and $g(u(0,t))$, the boundary-value-dependent gains are given by

$$k(x,y,u(0,t)) = -g(u(0,t))e^{(g(u(0,t))+b(u(0,t)))(x-y)} \tag{4}$$

$$l(x,y,w(0,t)) = -g(w(0,t))e^{b(w(0,t))(x-y)} \tag{5}$$

where $w(x,t)$ is assumed to be sufficiently smooth and is the state of a first-order hyperbolic target system on the domain $0 \le x \le 1$ at time $0 \le t < \infty$, with initial condition $w_0(x) = w(x,0)$. The gain (4) was found by setting $b = b(u(0,t))$ and $g = g(u(0,t))$ in the results of Ref. [26, example 2.1], while Eq. (5) was found following the general gain scheduled PDE backstepping design steps, i.e., assume b, g constant and find $l(x,y)$ using PDE backstepping tools, then substitute $b(\cdot)$, $g(\cdot)$. Similar to Ref. [26, example 2.1], the boundary controller is chosen as

$$u(1,t) = -\int_0^1 g(u(0,t))e^{(g(u(0,t))+b(u(0,t)))(1-y)}u(y,t)\,dy. \tag{6}$$

When b and g are constants the closed-loop system is equivalent to the exponentially stable target system $w_t(x,t) = w_x(x,t)$, $w(1,t) = 0$, whereas for general $b(\cdot)$ and $g(\cdot)$ the target system is

$$w_t(x,t) = w_x(x,t) - w_x(0,t)\int_0^x l_3(x,y,w(0,t))w(y,t)\,dy \tag{7}$$

$$w(1,t) = 0 \tag{8}$$

where $l_3(x,y,w(0,t))$ denotes the partial derivative of $l(x,y,w(0,t))$ with respect to $w(0,t)$, which for this particular problem is given by

$$l_3(x,y,w(0,t)) = -\left[g(w(0,t))b'(w(0,t))(x-y) + g'(w(0,t))\right]$$
$$\times e^{b(w(0,t))(x-y)} \tag{9}$$

The main result of this section is that the gain scheduling based nonlinear controller is locally exponentially stabilizing with respect to the appropriate norm. In the context of gain scheduling, the "continuously scheduled" controller is locally exponentially stabilizing independent of the magnitude of the rate of change of the scheduling signal $u(0,t)$. Note that this work is done with functions in H^1 space.

Definition 2.1. Let $\Gamma(t)$ denote the norm of the state of a dynamic system at time t. The equilibrium at the origin is said to be locally exponentially stable if there exist positive constants M, m, and γ such that for all initial states such that $\Gamma_0 < \gamma$, the following holds:

$$\Gamma(t) \le M\Gamma_0 e^{-mt}, \quad \forall t \ge 0 \tag{10}$$

Theorem 2.1. Consider the closed-loop system consisting of the plant Eq. (1) and the boundary controller Eq. (6), and let

$$\Omega(t) = u(0,t)^2 + \|u(t)\|^2 + \|u_x(t)\|^2 \tag{11}$$

denote its norm with respect to x at time t. The equilibrium $u \equiv 0$ of the closed-loop system is locally exponentially stable.

2.1 Proof of Theorem 2.1. The proof of Theorem 2.1 requires finding the stability properties of the equilibrium $w \equiv 0$ of the target system (7) and (8), then relating those properties to the closed-loop system (1) and (6) in the u-variable. First, results for the transformations and norms relating the systems are presented. Next a Lyapunov analysis is done to determine the stability of the equilibrium $w \equiv 0$ of the target system. The proof is completed by relating the results of the Lyapunov analysis in the w-variable to the u-variable using the system norms and the transformations.

The transformations $u \mapsto w$ and $w \mapsto u$ given by Eqs. (2)–(5) are consistent (one is the inverse of the other). This is shown by considering the partial derivative with respect to x of Eq. (2) with gain Eq. (4), which can be written as $u'(x,t) = b(u(0,t)) u(x,t) + w'(x,t) - [b(u(0,t)) + g(u(0,t))] w(x,t)$ and can be viewed as a linear ordinary differential equation (ODE) in x with solution given by Eqs. (3) and (5). Also, the partial derivative with respect to x of Eq. (3), with gain Eq. (5) can be written as $w'(x,t) = [g(w(0,t)) + b(w(0,t))] w(x,t) + u(x,t)' - b(u(0,t)) u(x,t)$, which can be viewed as a linear ODE in x with solution given by Eqs. (2) and (4). This establishes the direct and inverse transformations are consistent. The following lemma establishes that the direct transformation and its inverse relate the plant and target system PDEs under consideration.

Lemma 2.1. Let the functions $u(x,t)$ and $w(x,t)$ be related by Eqs. (2)–(5). The function $u(x,t)$ satisfies the nonlinear system (1) with boundary control (6) if and only if the function $w(x,t)$ satisfies the target system (7) and (8).

Proof. Substituting Eq. (3) into Eq. (1) and grouping terms gives

$$0 = u_t(x,t) - u_x(x,t) - g(u(0,t))e^{b(u(0,t))x}u(0,t)$$

$$= w_t(x,t) - w_x(x,t) + w_x(0,t)\int_0^x l_3(x,y,w(0,t))w(y,t)\,dy \quad (12a)$$

$$- \int_0^x \big\{ l_x(x,y,w(0,t)) + l_y(x,y,w(0,t)) \big\} w(y,t)\,dy \quad (12b)$$

$$- \big\{ l(x,0,w(0,t)) + g(w(0,t))e^{b(w(0,t))x} \big\} w(0,t) \quad (12c)$$

The expression in Eq. (12a) is satisfied by Eq. (7), and the braced expressions in Eqs. (12b) and (12c) are equal to zero given the inverse gain kernel Eq. (5). Substituting Eq. (3) into Eq. (6) gives

$$w(1,t) = \int_0^1 \Big\{ l(1,y,w(0,t)) - k(1,y,w(0,t))$$

$$- \int_y^1 k(1,\xi,w(0,t))l(\xi,y,w(0,t))\,d\xi \Big\} w(y,t)\,dy \quad (13)$$

which is zero given Eqs. (4) and (5).

Lemma 2.2. *Consider the target system (7) and (8), with the Lyapunov function candidate*

$$V(t) = \int_0^1 (1+x)w^2(x,t)\,dx + \int_0^1 (1+x)w_x^2(x,t)\,dx \quad (14)$$

There exists a positive constant $\mathcal{V}$ such that if $V_0 \le \mathcal{V}$ then

$$\dot{V}(t) \le -\frac{1}{4}V(t), \quad \forall t \ge 0 \quad (15)$$

Proof. The temporal derivative of Eq. (14) is

$$\dot{V}(t) = 2\int_0^1 (1+x)w(x,t)w_t(x,t)\,dx$$

$$+ 2\int_0^1 (1+x)w_x(x,t)w_{xt}(x,t)\,dx \quad (16)$$

where $w_t(x,t)$ is given in Eq. (7), and the $w_x(x,t)$-system is given by

$$w_{xt}(x,t) = w_{xx}(x,t) - w_x(0,t)l_3(x,x,w(0,t))w(x,t)$$

$$- w_x(0,t)\int_0^x l_{13}(x,y,w(0,t))w(y,t)\,dy \quad (17)$$

$$w_x(1,t) = w_x(0,t)\int_0^1 l_3(1,y,w(0,t))w(y,t)\,dy \quad (18)$$

with Eq. (17) found by taking the partial derivative with respect to x of Eq. (7), and Eq. (18) found by evaluating Eq. (7) at $x = 1$ with $w_t(1,t) = 0$ from Eq. (8), where $l_{13}(x,y,w(0,t))$ is used to denote the partial derivative of $l_3(x,y,w(0,t))$ with respect to x. Using Eqs. (7) and (17) to substitute for $w_t(x,t)$ and $w_{xt}(x,t)$, Eq. (16) can be written as

$$\dot{V}(t) = 2\int_0^1 (1+x)w(x,t)\Big\{ w_x(x,t) - w_x(0,t)\int_0^x l_3(x,y,w(0,t))w(y,t)\,dy \Big\}dx$$

$$+ 2\int_0^1 (1+x)w_x(x,t)\Big\{ w_{xx}(x,t) - w_x(0,t)l_3(x,x,w(0,t))w(x,t) - w_x(0,t)\int_0^x l_{13}(x,y,w(0,t))w(y,t)\,dy \Big\}dx$$

$$= w^2(1,t) - w^2(0,t) - ||(w(t)||^2 + w_x^2(1,t) - w_x^2(0,t) - ||(w_x(t)||^2$$

$$- 2w_x(0,t)\int_0^1 (1+x)w(x,t)\int_0^x l_3(x,y,w(0,t))w(y,t)\,dy\,dx$$

$$- 2w_x(0,t)\int_0^1 (1+x)w_x(x,t)l_3(x,x,w(0,t))w(x,t)\,dx$$

$$- 2w_x(0,t)\int_0^1 (1+x)w_x(x,t)\int_0^x l_{13}(x,y,w(0,t))w(y,t)\,dy\,dx \quad (19)$$

where integration by parts was used to resolve the integrals $\int_0^1 (1+x)w(x,t)w_x(x,t)\,dx$ and $\int_0^1 (1+x)w_x(x,t)w_{xx}(x,t)\,dx$. Using Eqs. (8) and (18) to substitute for $w(1,t)$ and $w_x(1,t)$ and taking the absolute value of the sign-indefinite terms, Eq. (19) can be bounded by

$$\dot{V}(t) \le -w^2(0,t) - w_x^2(0,t) - ||w(t)||^2 - ||w_x(t)||^2 \quad (20a)$$

$$+ 2\left(w_x(0,t)\int_0^1 l_3(1,y,w(0,t))w(y,t)\,dy \right)^2 \quad (20b)$$

Journal of Dynamic Systems, Measurement, and Control

$$+ 2\left|w_x(0,t)\int_0^1 (1+x)w(x,t)\int_0^x l_3(x,y,w(0,t))w(y,t)\,dy\,dx\right|$$

$$(20c)$$

$$+ 2\left|w_x(0,t)\int_0^1 (1+x)l_3(x,x,w(0,t))w(x,t)w_x(x,t)\,dx\right| \quad (20d)$$

$$+ 2\left|w_x(0,t)\int_0^1 (1+x)w_x(x,t)\int_0^x l_{13}(x,y,w(0,t))w(y,t)\,dy\,dx\right|$$

$$(20e)$$

Given that $b(\cdot)$ and $g(\cdot)$ are continuously differentiable functions, the term in Eq. (20b) can be bounded in the form

$$2\left(w_x(0,t)\int_0^1 l_3(1,y,w(0,t))w(y,t)\,dy\right)^2$$
$$\le 2w_x^2(0,t)[a_1 + \alpha_1(|w(0,t)|)]^2 \|w(t)\|^2 \quad (21)$$

the term in Eq. (20c) can be bounded in the form

$$2\left|w_x(0,t)\int_0^1 (1+x)w(x,t)\int_0^x l_3(x,y,w(0,t))w(y,t)\,dy\,dx\right|$$
$$\le \frac{1}{4}w_x^2(0,t) + 16[a_1 + \alpha_1(|w(0,t)|)]^2 \|w(t)\|^4 \quad (22)$$

the term in Eq. (20d) can be bounded in the form

$$2\left|w_x(0,t)\int_0^1 (1+x)l_3(x,x,w(0,t))w(x,t)w_x(x,t)\,dx\right|$$
$$\le \frac{1}{4}w_x^2(0,t) + 16[a_2 + \alpha_2(|w(0,t)|)]^2 \|w_x(t)\|^4 \quad (23)$$

and the term in Eq. (20e) can be bounded in the form

$$2\left|w_x(0,t)\int_0^1 (1+x)w_x(x,t)\int_0^x l_{13}(x,y,w(0,t))w(y,t)\,dy\,dx\right|$$
$$\le \frac{1}{4}w_x^2(0,t) + 16[a_3 + \alpha_3(|w(0,t)|)]^2 \|w_x(t)\|^4 \quad (24)$$

where a_i, $i=1,2,3$ are positive constants defined as

$$a_1 = |g'(0)|e^{|b(0)|} + |g(0)||b'(0)|e^{|b(0)|}$$
$$a_2 = |g'(0)|$$
$$a_3 = |g'(0)||b(0)|e^{|b(0)|} + |g(0)||b(0)||b'(0)|e^{|b(0)|}$$

and $\alpha_i(\cdot)$ are class $\mathcal{K}_\infty$ functions chosen as

$$\alpha_1(|w(0,t)|) \ge |g'(w(0,t))|e^{|b(w(0,t))|}$$
$$+ |g(w(0,t))||b'(w(0,t))|e^{|b(w(0,t))|} - a_1$$
$$\alpha_2(|w(0,t)|) \ge |g'(w(0,t))| - a_2$$
$$\alpha_3(|w(0,t)|) \ge |g'(w(0,t))||b(w(0,t))|e^{|b(w(0,t))|}$$
$$+ |g(w(0,t))||b(w(0,t))||b'(w(0,t))|e^{|b(w(0,t))|} - a_3$$

Using the bounds in Eqs. (21)–(24), the Agmon inequality bound $|w(0,t)| \le \|w_x(t)\| \le \sqrt{V(t)}$, and defining the class $\mathcal{K}_\infty$ functions

$$\beta_1\left(\sqrt{V}\right) = \left[a_1 + \alpha_1\left(\sqrt{V}\right)\right]^2 V$$

$$\beta_2\left(\sqrt{V}\right) = \left\{\left[a_2 + \alpha_2\left(\sqrt{V}\right)\right]^2 + \left[a_3 + \alpha_3\left(\sqrt{V}\right)\right]^2\right\} V$$

the inequality in Eq. (20) can be bounded by

$$\dot{V}(t) \le -w^2(0,t) - \left\{\frac{1}{4} - 2\beta_1\left(\sqrt{V(t)}\right)\right\}w_x^2(0,t)$$
$$- \left\{1 - 16\beta_1\left(\sqrt{V(t)}\right)\right\}\|w(t)\|^2 - \left\{1 - 16\beta_2\left(\sqrt{V(t)}\right)\right\}$$
$$\times \|w_x(t)\|^2 \quad (25)$$

Then for

$$V_0 \le \mathcal{V} = \min\left\{\beta_1^{-1}\left(\frac{1}{8}\right)^2, \beta_1^{-1}\left(\frac{1}{32}\right)^2, \beta_2^{-1}\left(\frac{1}{32}\right)^2\right\}$$

the expression in Eq. (25) can be bounded by

$$\dot{V}(t) \le -\frac{1}{2}\left(\|w(t)\|^2 + \|w_x(t)\|^2\right) \le -\frac{1}{4}V(t) \quad (26)$$

Given that the transformations between plant and target system are consistent, along with the results of Lemma 2.1 shows the existence of transformations relating the closed-loop system (1) and (6) and the target system (7) and (8).

The transformations will now be used to relate the Lyapunov function to the norm of the target system denoted by

$$\Psi(t) = \|w(t)\|^2 + \|w_x(t)\|^2 \quad (27)$$

and then to the norm Eq. (11) of the closed-loop system. Note that the Lyapunov function Eq. (14) is upper and lower bounded by

$$\Psi(t) \le V(t) \le 2\Psi(t) \quad (28)$$

which can be seen by considering the quantity $(1+x)$ in Eq. (14), and setting x to zero to produce the lower bound and one to produce the upper bound in Eq. (28). Stability of the equilibrium $w \equiv 0$ of the target system can now be stated having related the target system norm to the Lyapunov function. Equation (26) in Lemma 2.2 implies

$$V(t) \le V_0 e^{-t/4}, \quad \forall t \ge 0 \quad (29)$$

Then from Eqs. (28) and (29), $\Psi(t) \le V(t) \le V_0 e^{-t/4} \le 2\Psi_0 e^{-t/4}$ for $\Psi_0 \le V_0$, therefore, the equilibrium $w \equiv 0$ of the target system (7) and (8) is locally exponentially stable.

Lemma 2.3. *There exist class $\mathcal{K}_\infty$ functions $\delta(\cdot)$ and $\rho(\cdot)$ such that*

$$\Psi(t) \le \delta(\Omega(t)) \quad (30)$$

and

$$\Omega(t) \le \rho(\Psi(t)) \quad (31)$$

Proof. The inequality in Eq. (30) is established as follows. The terms $\|w(t)\|^2$ and $\|w_x(t)\|^2$ in Eq. (27) can be bounded by:

$$\|w(t)\|^2 \le \|u(t)\|^2 + \max_{0\le y\le x\le 1}|k(x,y,u(0,t))|^2\|u(t)\|^2 \quad (32)$$

and

$$\|w_x(t)\|^2 \le \|u_x(t)\|^2 + \max_{0\le x\le 1}|k(x,x,u(0,t))|^2\|u(t)\|^2$$
$$+ \max_{0\le y\le x\le 1}|k_x(x,y,u(0,t))|^2\|u(t)\|^2 \quad (33)$$

Using Eqs. (32) and (33), and given that $b(\cdot)$ and $g(\cdot)$ are continuously differentiable, Eq. (27) can be bounded by

$$\Psi(t) = \|w(t)\|^2 + \|w_x(t)\|^2 \leq \left(1 + \max_{0 \leq y \leq x \leq 1}|k(x,y,u(0,t))|^2 + \max_{0 \leq x \leq 1}|k(x,x,u(0,t))|^2 + \max_{0 \leq y \leq x \leq 1}|k_x(x,y,u(0,t))|^2\right)\|u(t)\|^2 + \|u_x(t)\|^2$$

$$\leq \left(1 + g(u(0,t))^2 e^{2(|g(u(0,t))|+|b(u(0,t))|)} + g(u(0,t))^2 + g(u(0,t))^2(|g(u(0,t))| + |b(u(0,t))|)^2 e^{2(|g(u(0,t))|+|b(u(0,t))|)}\right)\|u(t)\|^2 + \|u_x(t)\|^2$$

$$\leq (1 + a_4 + \alpha_4(|u(0,t)|))\|u(t)\|^2 + \|u_x(t)\|^2 \tag{34}$$

where the positive constant a_4 is defined as

$$a_4 = g(0)^2 e^{2(|g(0)|+|b(0)|)} + g(0)^2 + g(0)^2(|g(0)| + |b(0)|)^2 e^{2(|g(0)|+|b(0)|)} \tag{35}$$

and $\alpha_4(\cdot)$ is a class $\mathcal{K}_\infty$ function chosen as

$$\alpha_4(|u(0,t)|) \geq g(u(0,t))^2 e^{2(|g(u(0,t))|+|b(u(0,t))|)} + g(u(0,t))^2$$
$$+ g(u(0,t))^2(|g(u(0,t))|$$
$$+ |b(u(0,t))|)^2 e^{2(|g(u(0,t))|+|b(u(0,t))|)} - a_4 \tag{36}$$

Then Eq. (34) can be bounded by

$$\Psi(t) \leq (1 + a_4 + \alpha_4(|u(0,t)|))\left(\|u(t)\|^2 + \|u_x(t)\|^2\right)$$

$$\Omega(t) = u(0,t)^2 + \|u(t)\|^2 + \|u_x(t)\|^2$$

$$\leq \|w_x(t)\|^2 + \left(1 + \max_{0 \leq y \leq x \leq 1}|l(x,y,w(0,t))|^2 + \max_{0 \leq x \leq 1}|l(x,x,w(0,t))|^2 + \max_{0 \leq y \leq x \leq 1}|l_x(x,y,w(0,t))|^2\right)\|w(t)\|^2 + \|w_x(t)\|^2$$

$$\leq \left(1 + g(w(0,t))^2 e^{2|b(w(0,t))|} + g(w(0,t))^2 + g(w(0,t))^2 b(w(0,t))^2 e^{2|b(w(0,t))|}\right)\|w(t)\|^2 + 2\|w_x(t)\|^2$$

$$\leq (1 + a_5 + \alpha_5(|w(0,t)|))\|w(t)\|^2 + 2\|w_x(t)\|^2 \tag{40}$$

where the positive constant a_5 is defined as

$$a_5 = g(0)^2 e^{2|b(0)|} + g(0)^2 + g(0)^2 b(0)^2 e^{2|b(0)|} \tag{41}$$

and $\alpha_5(\cdot)$ is a class $\mathcal{K}_\infty$ function chosen as

$$\alpha_5(|w(0,t)|) \geq g(w(0,t))^2 e^{2|b(w(0,t))|} + g(w(0,t))^2$$
$$+ g(w(0,t))^2 b(w(0,t))^2 e^{2|b(w(0,t))|} - a_5 \tag{42}$$

Then Eq. (40) can be bounded by

$$\Omega(t) \leq (2 + a_5 + \alpha_5(|w(0,t)|))\left(\|w(t)\|^2 + \|w_x(t)\|^2\right)$$
$$\leq \left(2 + a_5 + \alpha_5\left(\sqrt{\Psi(t)}\right)\right)\Psi(t) = \rho(\Psi(t)) \tag{43}$$

The proof of Theorem 2.1 is completed next. Let $\omega = \delta^{-1}(\mathcal{V}/2)$. Restricting the plant initial condition to $\Omega_0 \leq \omega$ implies that $V_0 \leq 2\Psi_0 \leq 2\delta(\Omega_0) \leq 2\delta(\omega) = \mathcal{V}$. Then based on the preceding discussion the norm $\Omega(t)$ of the closed-loop system can be bounded by

$$\Omega(t) \leq \rho(\Psi(t))$$
$$\leq \rho(V(t))$$
$$\leq \rho\left(V_0 e^{-t/4}\right)$$
$$\leq \rho\left(2\Psi_0 e^{-t/4}\right)$$
$$\leq \rho\left(2\delta(\Omega_0)e^{-t/4}\right) \tag{44}$$

$$\leq \left(1 + a_4 + \alpha_4\left(\sqrt{\Omega(t)}\right)\right)\Omega(t) = \delta(\Omega(t)) \tag{37}$$

The inequality in Eq. (31) is established as follows. The terms $\|u(t)\|^2$ and $\|u_x(t)\|^2$ in Eq. (11) can be bounded by:

$$\|u(t)\|^2 \leq \|w(t)\|^2 + \max_{0 \leq y \leq x \leq 1}|l(x,y,w(0,t))|^2\|w(t)\|^2 \tag{38}$$

and

$$\|u_x(t)\|^2 \leq \|w_x(t)\|^2 + \max_{0 \leq x \leq 1}|l(x,x,w(0,t))|^2\|w(t)\|^2$$
$$+ \max_{0 \leq y \leq x \leq 1}|l_x(x,y,w(0,t))|^2\|w(t)\|^2 \tag{39}$$

Using Eqs. (38) and (39), the bound $u(0,t) = w(0,t) \leq \|w_x(t)\|$, and given that $b(\cdot)$ and $g(\cdot)$ are continuously differentiable functions, Eq. (11) can be bounded by

Given that ρ and δ are continuous and have a linear growth at the origin, an exponential stability estimate in the form Eq. (10) is achieved for $\Omega(t)$.

3 Application to a String PDE

This section presents only the application of the gain scheduling based PDE backstepping techniques of Sec. 2 to the control design for a string with Kelvin–Voigt damping and boundary-displacement-dependent free-end nonlinearity. No theoretical results or stability analysis for a closed-loop system are presented here, but they can be pursued using the tools developed in Sec. 2.1. Conditions under which the results of this section would hold locally, proposed based on the results of Theorem 2.1, are summarized at the end of this section. The merits of the designs in this section are illustrated by simulation in Sec. 4.

Consider the string model given by

$$\varepsilon u_{tt}(x,t) = \left(1 + d\frac{\partial}{\partial t}\right)u_{xx}(x,t) \tag{45}$$

$$u_x(0,t) = f(u(0,t)) \tag{46}$$

where $u(x,t)$ denotes the displacement with initial conditions $u_0(x) = u(x,0)$ and $\dot{u}_0(x) = u_t(x,0)$, d is the Kelvin–Voigt damping coefficient, and ε is the inverse of the nondimensional stiffness. The string is actuated at $x = 1$ through the force boundary input $u_x(1,t)$. The boundary-displacement-dependent function $f(\cdot)$, representing a free-end nonlinearity, is an arbitrary continuously differentiable function with $f(0) = 0$. Depending on the sign of $f'(u(0,t)) = df(u(0,t))/du(0,t)$ the nonlinear force can

have either positive stiffness $(f' > 0)$, or negative stiffness $(f' < 0)$, i.e., "antistiffness," which is destabilizing. This work will consider systems with $f' < 0$ (at least locally), where control is required to stabilize the equilibrium $u \equiv 0$ of the closed-loop system. A gain scheduling based PDE backstepping design is chosen in hopes of improving on linearization based results, both in the transient response and in the range of stability with respect to initial conditions.

Given that $f(u(0,t))$ is continuously differentiable and $f(0) = 0$, $f(\cdot)$ can be written in the necessary LPV form $\bar{f}(u(0,t))u(0,t)$, where the nonlinearity can be given explicitly, modeled, or approximated such that $u(0,t)$ can be factored out. The results in Ref. [27, Sec. 3] are for an undamped string $(d = 0)$ with $\varepsilon = 1$, and linear destabilizing force, i.e., constant $\bar{f}$. The presence of KV damping and nonunity ε in this problem do not change the design compared to Ref. [27, Sec. 3]. The gain scheduling based backstepping transformations are then Eqs. (2) and (3), where in the present problem with $\bar{f}(u(0,t))$ the boundary-displacement-dependent gains are given by

$$k(x, y, u(0,t)) = [\bar{f}(u(0,t)) - c_0]e^{-\bar{f}(u(0,t))(x-y)} \tag{47}$$

$$l(x, y, w(0,t)) = [\bar{f}(w(0,t)) - c_0]e^{-c_0(x-y)} \tag{48}$$

where $w(x,t)$ is the state of a target system given by a wave equation with KV damping on the domain $0 \le x \le 1$ at time $0 \le t < \infty$ with initial conditions $w_0(x) = w(x,0)$, $\dot{w}_x(x) = w_t(x,0)$. The constant $c_0 > 0$ is a design parameter of the target system. Similar to Ref. [27] the boundary controller is chosen as

$$u_x(1,t) = [\bar{f}(u(0,t)) - c_0]u(1,t)$$
$$- \bar{f}(u(0,t))[\bar{f}(u(0,t)) - c_0] \int_0^1 e^{-\bar{f}(u(0,t))(1-y)}u(y,t)\,dy$$
$$- c_1 u_t(1,t) + c_1[\bar{f}(u(0,t)) - c_0] \int_0^1 e^{-\bar{f}(u(0,t))(1-y)}u_t(y,t)\,dy \tag{49}$$

where $c_1 > 0$ is a second design parameter of the target system. Here Eqs. (47)–(49) were found by substituting $\bar{f} = \bar{f}(u(0,t))$ into Ref. [27], Eqs. (6), (7), and (4), respectively (to be exact, $-q \equiv f(u(0,t))$, $c_1 \equiv c_0$ and $c_2 \equiv c_1$). When $\bar{f}$ is constant, the closed-loop system (45), (46), and (49) is equivalent to the exponentially stable target system [27–34]

$$\varepsilon w_{tt}(x,t) = \left(1 + d\frac{\partial}{\partial t}\right)w_{xx}(x,t) \tag{50}$$

$$w_x(0,t) = c_0 w(0,t) \tag{51}$$

$$w_x(1,t) = -c_1 w_t(1,t) \tag{52}$$

For general $\bar{f}(\cdot)$ the target system is

$$\varepsilon w_{tt}(x,t) = \left(1 + d\frac{\partial}{\partial t}\right)w_{xx}(x,t)$$
$$- 2\varepsilon w_t(0,t) \int_0^x l_3(x, y, w(0,t))w_t(y,t)\,dy$$
$$- \varepsilon \int_0^x \left[w_t(0,t)^2 l_{33}(x, y, w(0,t)) + w_{tt}(0,t)l_3(x, y, w(0,t))\right]$$
$$\times w(y,t)\,dy \tag{53}$$

with boundary conditions (51) and (52), where $l_3(x, y, w(0,t))$ denotes the partial derivative of $l(x, y, w(0,t))$ with respect to $w(0,t)$ and $l_{33}(x, y, w(0,t))$ denotes the second partial derivative of $l(x, y, w(0,t))$ with respect to $w(0,t)$, which for this particular problem are given by

$$l_3(x, y, w(0,t)) = \bar{f}'(w(0,t))e^{-c_0(x-y)} \tag{54}$$

$$l_{33}(x, y, w(0,t)) = \bar{f}''(w(0,t))e^{-c_0(x-y)} \tag{55}$$

The motion planning and tracking results of Refs. [29,30], which were developed only for $\bar{f} \equiv 0$, can also be extended to Eqs. (45) and (46) using gain scheduling techniques. The results for general $\bar{f}(\cdot)$ are found following the design techniques in Refs. [29,30] but with transformations (2), (3), (47), and (48). The motion planning reference solution is

$$u^r(x,t) = w^r(x,t) + [\bar{f}(w^r(0,t)) - c_0] \int_0^x e^{-c_0(x-y)}w^r(y,t)\,dy \tag{56}$$

where $w^r(x,t)$ is the reference solution for Eqs. (50) and (51), which for the tip displacement reference trajectory

$$u^r(0,t) = A_u \sin(\omega_u t) \tag{57}$$

is given by Ref. [29,30]

$$w^r(x,t) = \frac{A_u}{2}\left[e^{\hat{\beta}(\omega_u)x}\sin(\omega_u t + \beta(\omega_u)x) + e^{-\hat{\beta}(\omega_u)x}\sin(\omega_u t - \beta(\omega_u)x)\right]$$
$$- \frac{c_0 A_u}{2}\left\{\gamma(\omega_u)\left[e^{\hat{\beta}(\omega_u)x}\cos(\omega_u t + \beta(\omega_u)x) - e^{-\hat{\beta}(\omega_u)x}\cos(\omega_u t - \beta(\omega_u)x)\right]\right.$$
$$\left. - \hat{\gamma}(\omega_u)\left[e^{\hat{\beta}(\omega_u)x}\sin(\omega_u t + \beta(\omega_u)x) - e^{-\hat{\beta}(\omega_u)x}\sin(\omega_u t - \beta(\omega_u)x)\right]\right\} \tag{58}$$

which generates the reference trajectory $w^r(0,t) = A_u \sin(\omega_u t)$ for a desired amplitude A_u and frequency ω_u. The functions $\beta(\cdot)$, $\hat{\beta}(\cdot)$, $\gamma(\cdot)$, and $\hat{\gamma}(\cdot)$ are defined as

$$\beta(n) = n\sqrt{\varepsilon}\sqrt{\frac{\sqrt{1 + n^2 d^2} + 1}{2(1 + n^2 d^2)}} \tag{59}$$

$$\hat{\beta}(n) = n\sqrt{\varepsilon}\sqrt{\frac{\sqrt{1 + n^2 d^2} - 1}{2(1 + n^2 d^2)}} \tag{60}$$

$$\gamma(n) = \frac{1}{n\sqrt{\varepsilon}}\sqrt{\frac{\sqrt{1 + n^2 d^2} + 1}{2}} \tag{61}$$

$$\hat{\gamma}(n) = \frac{1}{n\sqrt{\varepsilon}} \sqrt{\frac{\sqrt{1+n^2 d^2}-1}{2}} \qquad (62)$$

The force boundary input for motion planning is

$$
\begin{aligned}
u_x^r(1,t) = {} & w_x^r(1,t) + [\bar{f}(w^r(0,t)) - c_0]w^r(1,t) \\
& - c_0[\bar{f}(w^r(0,t)) - c_0] \int_0^1 e^{-c_0(1-y)} w^r(y,t)\,dy
\end{aligned} \qquad (63)
$$

and the tracking boundary controller is

$$
\begin{aligned}
u_x(1,t) = {} & [\bar{f}(u(0,t)) - c_0]u(1,t) \\
& - \bar{f}(u(0,t))[\bar{f}(u(0,t)) - c_0] \int_0^1 e^{-\bar{f}(u(0,t))(1-y)} u(y,t)\,dy \\
& - c_1 u_t(1,t) \\
& + c_1[\bar{f}(u(0,t)) - c_0] \int_0^1 e^{-\bar{f}(u(0,t))(1-y)} u_t(y,t)\,dy \\
& + w_x^r(1,t) + c_1 w_t^r(1,t)
\end{aligned}
$$
$$(64)$$

The string boundary controllers (49) and (64) require slope/force actuation at the base but can also be written in a form that requires displacement actuation. When combined with full state observers [27,28], the output-feedback controllers require sensing of the free-end displacement and velocity.

Following the results of Theorem 2.1, the initial conditions $u_0(x)$, $\dot{u}_0(x)$, $u_0(x) - u_0^r(x)$, and $\dot{u}_0(x) - \dot{u}_0^r(x)$, along with the reference trajectory $u^r(0,t)$ should be sufficiently small in the appropriate norms for the nonlinear controllers (49), and (64) to be exponentially stabilizing and for the reference solution (56) to hold. Such restrictions would seem to confine the operation to a linear region of $f(\cdot)$. Indeed, the advantage of using the nonlinear gain scheduled controls is impossible to quantify using the conservative analysis tools of Sec. 2.1. The advantage of gain scheduling based control over linearization based control is illustrated by simulations.

4 Simulations for the String

Simulations are done for the string (45), (46) with the stabilizing boundary controller (49) and tracking controller (64). The spatial and temporal step sizes are $\Delta x = \frac{1}{100}$ and $\Delta t = \frac{1}{100}$, respectively, the string parameters are $d = 0.08$ and $\varepsilon = 5$, and the controller parameters are $c_0 = 10$ and $c_1 = 0.99\sqrt{5}$. Figure 1 compares the softening nonlinearity $f(u(0,t)) = -\left[\frac{1}{200}u(0,t) + (2u(0,t))^3\right]$ used in simulations and its linear approximation $f'(0)u(0,t)$. The boundary-displacement-dependent interaction force has a weak linear region near the origin, which is then dominated by the cubic nonlinearity. The linear approximation about the origin underestimates the interaction force, i.e.,
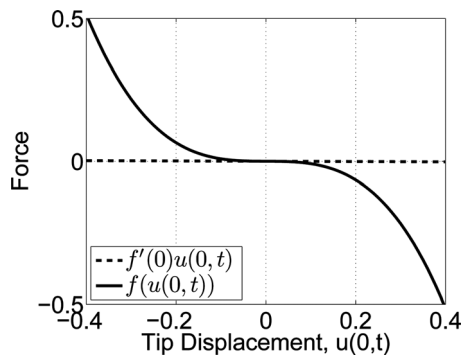

Fig. 1 Comparison of the nonlinearity $f(u(0,t))$ used in the string simulations, and its linear approximation $f'(0)u(0,t)$.

$|f'(0)u(0,t)| \leq |f(u(0,t))|$ for all $u(0,t)$. In fact, any linear approximation would eventually underestimate a superlinear nonlinearity, which tend to be the most difficult to compensate for.

Figure 2 compares the "energy" $E(t) = ||u_t(t)||^2 + ||u_x(t)||^2$, tip displacement $u(0,t)$, and boundary control effort $u_x(1,t)$ of the closed-loop system for the linearization based controller and the gain scheduling based nonlinear controller. The string is initialized with zero initial velocity and the initial displacement profile $u_0(x) = u_0(0)(1-x)$ for the initial tip displacements $u_0(0) = \{0.1, 0.3, 0.347, 0.363\}$. For sufficiently small initial conditions $(u_0(0) = 0.1)$, which lie in the linear region of the interaction force, both cases perform equally well. For intermediate initial conditions $(u_0(0) = 0.3)$ both cases stabilize the string with the gain scheduling based nonlinear controller achieving an improved transient response and slightly quicker settling time. When $u_0(0) = 0.347$, which is the largest initial condition for which the linearization based controller stabilizes the origin, the gain scheduling based nonlinear controller clearly outperforms the linearization based controller in both transient response and settling time. When $u_0(0) = 0.363$, which is the largest initial condition for which the gain scheduling based nonlinear controller stabilizes the origin, the linearization based controller can no longer stabilize the origin while the gain scheduling based nonlinear controller must work hard to keep the nonlinearity from pulling the tip away from the origin. The simulations show that—for a nonlinearity where the linearization underestimates the force—the gain scheduled based nonlinear controller outperforms the linearization based controller when the tip begins to operate in a sufficiently strong region of the nonlinear interaction force. The transient energy of the closed-loop system with gain scheduling based nonlinear control tends to be higher because of the increased control effort required for improved performance.

Figure 3 compares the performance of the linearization based controller and gain scheduling based nonlinear controller, when the goal is to generate and track the reference trajectory $u^r(0,t) = 0.3\sin \pi t$. The string is initialized with zero initial conditions. The gain scheduling based nonlinear controller is able to generate and track the sinusoid, with a small negative error in the mean. The negative error in the mean is caused by $u(0,t)$ interacting most with the nonlinearity through a negative peak of the sinusoid first. This is confirmed by simulations with $u^r(0,t) = -0.3\sin \pi t$ where the tip displacement interacts most with the nonlinearity through a positive peak of the sinusoid first, and the resulting error in the mean is positive. The negative mean causes a stronger interaction force for the negative peaks, which in turn causes phase tracking errors between them and the positive peaks. Conversely, the negative mean causes a weaker interaction force for the positive peaks, which allows for better tracking from positive to negative peaks. The plot also shows how the linearization based controller begins to generate and track the reference trajectory with the same error in the mean, but ultimately cannot compensate for the destabilizing force caused by increased interaction with the negative peaks. As with the stabilization simulations, the controllers have comparable performance for small reference amplitudes and the gain scheduled controller outperforms the linearization based controller when the amplitude increases, and neither controller can stabilize the reference trajectory when the reference amplitude is too large.

5 Application to the Shear Beam PDE

This section presents only the application of the gain scheduling based PDE backstepping techniques of Sec. 2 to the control design for the shear beam with Kelvin–Voigt damping and boundary-displacement-dependent free-end nonlinearity. No theoretical results or stability analysis for a closed-loop system are presented here, but they can be pursued using the tools developed in Sec. 2.1. Conditions under which the results of this section would hold locally, proposed based on the results of Theorem 2.1, are
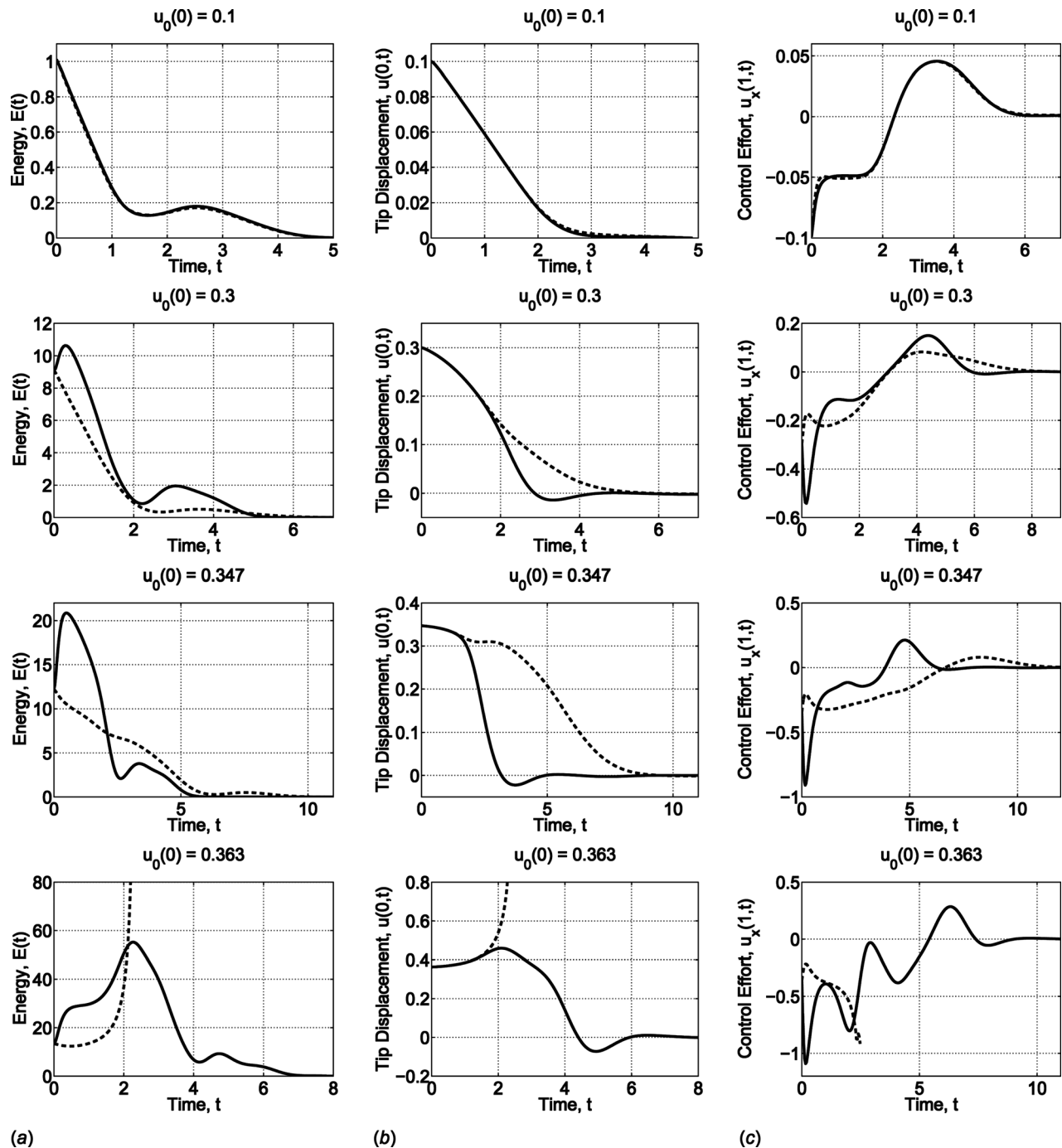
Fig. 2 String simulation results for the closed-loop system for boundary control using linearization based controller (dashed) and gain scheduling based nonlinear controller (solid), for initial tip displacements $u_0(0) = \{0.1, 0.3, 0.347, 0.363\}$. The plots compare (a) the energy $E(t) = ||u_t(t)||^2 + ||u_x(t)||^2$, (b) the tip displacement $u(0, t)$, and (c) the boundary control effort $u_x(1, t)$.

summarized at the end of the section. The merits of the results of this section are illustrated by simulation in Sec. 6.

Consider the Timoshenko beam model with Kelvin–Voigt damping and boundary-displacement-dependent free-end nonlinearity given as the coupled wave equations

$$\varepsilon u_{tt}(x,t) = \left(1 + d\frac{\partial}{\partial t}\right)\{u_{xx}(x,t) - \alpha_x(x,t)\} \qquad (65)$$

$$\mu\varepsilon\alpha_{tt}(x,t) = \left(1 + d\frac{\partial}{\partial t}\right)\{\varepsilon\alpha_{xx}(x,t) + a(u_x(x,t) - \alpha(x,t))\} \qquad (66)$$

$$u_x(0,t) = \alpha(0,t) + f(u(0,t)) \qquad (67)$$

$$\alpha_x(0,t) = 0 \qquad (68)$$

where the states $u(x,t)$ and $\alpha(x,t)$ denote the displacement and deflection angle with initial conditions $u_0(x) = u(x,0)$, $\dot{u}_0(x) = u_t(x,0)$, $\alpha_0(x) = \alpha(x,0)$ and $\dot{\alpha}_0(x) = \alpha_t(x,0)$. The positive constants a, ε, and μ are nondimensional parameters of the beam as defined in Refs. [35,36]. The $x = 0$ boundary conditions Eqs. (67), and (68) represent a free-end with nonlinear interaction force, and the beam is actuated at the end $x = 1$ through the boundary inputs $u_x(1,t)$ and $\alpha(1,t)$. The shear beam model can be
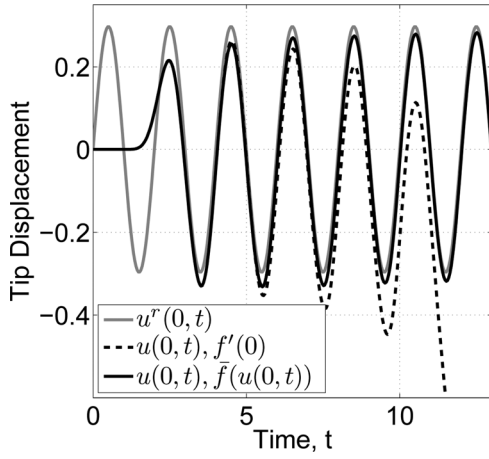
Fig. 3 String simulation results comparing the tip displacement $u(0,t)$ and reference trajectory $u^r(0,t)$ when boundary control is applied with linearization based control and gain scheduling based nonlinear control.

written as a singular perturbation $(\mu = 0)$ of the Timoshenko beam model, and is given by

$$\varepsilon u_{tt}(x,t) = \left(1 + d\frac{\partial}{\partial t}\right)\{u_{xx}(x,t) - \alpha_x(x,t)\} \qquad (69)$$

$$0 = \varepsilon\alpha_{xx}(x,t) + a(u_x(x,t) - \alpha(x,t)) \qquad (70)$$

with boundary conditions (67) and (68) and boundary inputs $u_x(1,t)$, $\alpha(1,t)$. As with the string, $f(\cdot)$ is considered to be destabilizing, and a gain scheduling based PDE backstepping design is chosen to stabilize $u \equiv 0$, $\alpha \equiv 0$.

The results in Ref. [31, Sec. 3] are for an undamped $(d=0)$ shear beam with linear destabilizing force, i.e., constant $\bar{f}$. The presence of KV damping in this problem does not change the design, and the gain scheduling based backstepping transformations are Eqs. (2) and (3), where for the present problem with $\bar{f}(u(0,t))$ the boundary-displacement-dependent gains satisfy the partial integro-differential equations

$$k_{xx}(x,y,u(0,t)) = k_{yy}(x,y,u(0,t)) + b^2 k(x,y,u(0,t))$$
$$+ b^3 \int_y^x k(x,\xi,u(0,t))\sinh(b(\xi-y))\,d\xi$$
$$- b^3 \sinh(b(x-y)) \qquad (71)$$

$$k(x,x,u(0,t)) = -\frac{b^2}{2}x + \bar{f}(u(0,t)) - c_0 \qquad (72)$$

$$k_y(x,0,u(0,t)) = -b^2\cosh(bx) + b^2\int_0^x k(x,y,u(0,t))\cosh(by)\,dy$$
$$+ \bar{f}(u(0,t))k(x,0,u(0,t)) \qquad (73)$$

and

$$l_{xx}(x,y,w(0,t)) = l_{yy}(x,y,w(0,t)) - b^2 l(x,y,w(0,t))$$
$$- b^3 \int_y^x l(x,\xi,w(0,t))\sinh(b(\xi-y))\,d\xi$$
$$- b^3 \sinh(b(x-y)) \qquad (74)$$

$$l(x,x,w(0,t)) = -\frac{b^2}{2}x + \bar{f}(w(0,t)) - c_0 \qquad (75)$$

$$l_y(x,0,w(0,t)) = -b^2\cosh(bx) + c_0 l(x,0,w(0,t)) \qquad (76)$$

Here Eqs. (71)–(73) were found by substituting $-q \equiv \bar{f}(\cdot)$ in Eq. (3.9), of Ref. [31], while Eqs. (74)–(76) were found using gain scheduling based PDE backstepping techniques. Note that Eqs. (71)–(73), Eqs. (74)–(76) are families of PIDEs in independent variables (x,y), and parametrized by $u(0,t)$, $w(0,t)$. For each measured $u(0,t)$, $w(0,t)$ the PIDEs are solved and their solutions substituted appropriately. Given that $k(x,y,u(0,t))$ and $l(x,y,w(0,t))$ are implemented 'continuously,' then an alternative to numerically solving their respective PIDEs is to approximate the functions by the explicit first step of a symbolic recursion [31]. The first step of the recursion for the shear beam gains gives $k^0(x,y,u(0,t)) = \Pi(x,y,u(0,t))$ and $l^0(x,y,w(0,t)) = \Pi(x,y,w(0,t))$, where $\Pi(x,y,n) = -(b/2)[-\sinh(b(x-y)) + by\cosh(b(x-y))] + \bar{f}(n) - c_0$. Similar to Ref. [31, Sec. 3] the locally stabilizing boundary controllers are chosen as

$$u_x(1,t) = k(1,1,u(0,t))u(1,t) + \int_0^1 k_x(1,y,u(0,t))u(y,t)\,dy$$
$$- c_1 u_t(1,t) + c_1 \int_0^1 k(1,y,u(0,t))u_t(y,t)\,dy \qquad (77)$$

$$\alpha(1,t) = b\sinh(b)u(0,t) - b^2\int_0^1 \cosh(b(1-y))u(y,t)\,dy \qquad (78)$$

The boundary controller Eq. (77) was found by making substitutions, similar to those made for the string, into Eq. 3.7 of Ref. [31] while Eq. (78) is carried over from Refs. [31–34]. Numerical results in Ref. [34] show comparable performance of the boundary controllers when applied with the first step approximation $k^0(x,y,u(0,t))$ or with the numerical solution of Eqs. (71)–(73) Similar to the string, when $\bar{f}$ is constant the closed-loop system Eqs. (67)–(78) is equivalent to the exponentially stable target system Eqs. (50)–(52), and for general $\bar{f}(\cdot)$ the target system is Eqs. (51)–(53) with $l(x,y,w(0,t))$ given by the numerical solution of Eqs. (74)–(76), or approximated by $l^0(x,y,w(0,t))$.

The motion planning and tracking results of Refs. [29,30] can also be extended to Eqs. (67)–(70) using gain scheduling techniques. As with the string, previous motion planning and tracking results were developed only for $\bar{f} \equiv 0$. Results for general $\bar{f}(\cdot)$ are found following the techniques in Refs. [29,30] but with the transformations Eqs. (2), (3), (71)–(73), and (74)–(76) The gain scheduling based backstepping transformations for motion planning and tracking are

$$w(x,t) = u(x,t) + r(x,t) - \int_0^x k(x,y,u(0,t))u(y,t)\,dy \qquad (79)$$

$$u(x,t) = w(x,t) - r(x,t) + \int_0^x l(x,y,w(0,t))[w(y,t) - r(y,t)]\,dy \qquad (80)$$

where $k(x,y,u(0,t))$ and $l(x,y,w(0,t))$ are given by Eqs. (71)–(73) and (74)–(76), and $r(x,t)$ is the state of an auxiliary system governed by a second-order parabolic PDE forced by $\alpha^r(0,t)$. The motion planning reference solutions are

$$u^r(x,t) = w^r(x,t) - r(x,t)$$
$$+ \int_0^x l(x,y,w^r(0,t))[w^r(y,t) - r(y,t)]\,dy \qquad (81)$$

$$\alpha^r(x,t) = \cosh(bx)\alpha^r(0,t) + b\sinh(bx)u^r(0,t)$$
$$- b^2\int_0^x \cosh(b(x-y))u^r(y,t)\,dy \qquad (82)$$

where for the tip displacement and deflection angle reference trajectories Eq. (57) and

$$\alpha^r(0,t) = A_\alpha \sin(\omega_\alpha t) \qquad (83)$$

$w^r(x,t)$ is given by Eq. (58), and $r(x,t)$ is

$$r(x,t) = A_\alpha \left(f_1(x) - \int_0^x f_1(x-y)\phi(y)\,dy \right) \sin(\omega_\alpha t)$$
$$+ A_\alpha \left(f_2(x) - \int_0^x f_2(x-y)\phi(y)\,dy \right) \cos(\omega_\alpha t) \qquad (84)$$

with

$$f_1(x) = \gamma(\omega_\alpha) \sin(\beta(\omega_\alpha)x) \cosh(\hat{\beta}(\omega_\alpha)x)$$
$$+ \hat{\gamma}(\omega_\alpha) \cos(\beta(\omega_\alpha)x) \sinh(\hat{\beta}(\omega_\alpha)x) \qquad (85)$$

$$f_2(x) = -\gamma(\omega_\alpha) \cos(\beta(\omega_\alpha)x) \sinh(\hat{\beta}(\omega_\alpha)x)$$
$$+ \hat{\gamma}(\omega_\alpha) \sin(\beta(\omega_\alpha)x) \cosh(\hat{\beta}(\omega_\alpha)x) \qquad (86)$$

$$\phi(x) = -b \sinh(bx) + b \int_0^x k(x,y,u(0,t)) \sinh(by)\,dy \qquad (87)$$

where $\beta(\omega_\alpha)$, $\hat{\beta}(\omega_\alpha)$, $\gamma(\omega_\alpha)$, $\hat{\gamma}(\omega_\alpha)$ are given in Eqs. (59)–(62) The boundary inputs for motion planning are

$$u_x^r(1,t) = w_x^r(1,t) - r_x(1,t) + l(1,1,w^r(0,t))[w^r(1,t) - r(1,t)]$$
$$+ \int_0^1 l_x(1,y,w^r(0,t))[w^r(y,t) - r(y,t)]\,dy \qquad (88)$$

$$\alpha^r(1,t) = \cosh(b)\alpha^r(0,t) + b \sinh(b)u^r(0,t)$$
$$- b^2 \int_0^1 \cosh(b(1-y))u^r(y,t)\,dy \qquad (89)$$

and the tracking boundary controllers are

$$u_x(1,t) = k(1,1,u(0,t))u(1,t) + \int_0^1 k_x(1,y,u(0,t))u(y,t)\,dy$$
$$- c_1 u_t(1,t) + c_1 \int_0^1 k(1,y,u(0,t))u_t(y,t)\,dy + w_x^r(1,t)$$
$$+ c_1 w_t^r(1,t) - r_x(1,t) - c_1 r_t(1,t) \qquad (90)$$

$$\alpha(1,t) = \cosh(b)\alpha^r(0,t) + b \sinh(b)u(0,t)$$
$$- b^2 \int_0^1 \cosh(b(1-y))u(y,t)\,dy \qquad (91)$$

The beam boundary controllers (77), (78) and (90), (91) require actuation of the slope (or displacement) and bending moment at the base. When combined with full state observers [31–34], the output-feedback controllers require sensing of the free-end displacement and velocity.

Based on the results of Theorem 2.1, the initial conditions $u_0(x)$, $\dot{u}_0(x)$, $u_0(x) - u_0^r(x)$, and $\dot{u}_0(x) - \dot{u}_0^r(x)$, along with the reference trajectory $u^r(0,t)$ should be sufficiently small in the appropriate norms for the nonlinear controllers Eqs. (77), (78) and (90), (91) to be exponentially stabilizing and for the reference solutions Eqs. (81) and (82) to hold. Such restrictions would seem to confine the operation to a linear region of $f(\cdot)$. Since the advantage of using the nonlinear gain scheduled controls is impossible to quantify using the conservative analysis tools of Sec. 2.1, then the advantage of gain scheduling based control over linearization based control is illustrated by simulations in Sec. 6.

6 Simulations for the Timoshenko Beam

The Timoshenko beam control design in Refs. [33,34] is done using a singular perturbation approach to reduce it to the shear beam model, with the rest of the design being analogous to the

shear beam results in Refs. [31,32]. All results for the shear beam apply *approximately* to the Timoshenko beam, therefore the gain scheduling based designs for the shear beam also apply approximately to the Timoshenko beam.

Simulations are done for the Timoshenko beam Eqs. (65)–(68) with the stabilizing boundary controllers Eqs. (77) and (78) and tracking controllers Eqs. (90) and (91) using the numerical solution to the gain PIDE, Eqs. (71)–(73) The spatial and temporal step sizes are $\Delta x = \frac{1}{100}$ and $\Delta t = \frac{1}{50}$, respectively, the beam parameters are $a = 5$, $d = 0.1$, $\varepsilon = 10$, and $\mu = 0.02$, and the controller parameters are $c_0 = 10$ and $c_1 = 0.99\sqrt{10}$. String simulations were done with a superlinear nonlinearity which demanded a more aggressive control action. Beam simulations are done with a sublinear nonlinearity which demands a less aggressive control action. Figure 4 compares the nonlinearity $f(u(0,t)) = -Fu(0,t)/1 + (3u(0,t))^2$ for $F = 1$, where F is the linear strength of the force, and its linear approximation about the origin. The boundary-displacement-dependent interaction force has a linear region about the origin, which is then dominated by the quadratic nonlinearity in the denominator. The linear approximation **overestimates** the interaction force, i.e. $|f'(0)u(0,t)| \geq |f(u(0,t))|$ for all $u(0,t)$. This sublinear nonlinearity is easier to compensate for compared to superlinear nonlinearity used for the string since, though it may destabilize the origin, its strength decreases far from the origin and it can add two new stable equilibria at $|u(0,t)| > 0$.

Figure 5 compares the energy $E(t)$, tip displacement $u(0,t)$, and boundary control effort $u_x(1,t)$ of the closed-loop system for the linearization based controller and the gain scheduling based nonlinear controller. The beam is initialized with zero initial velocity and the initial displacement and deflection angle profiles $u_0(x) = \frac{3}{10}(1-x)^2$ and $\alpha_0(x) = -\frac{3}{5}(1-x)$, and the nonlinearity strength is varied as $F = \{0.1, 0.3, 0.53, 2, 2.8\}$. The goal of these simulations is to compare the two control implementations, as opposed to finding the best control parameters c_0 and c_1 for a particular F, therefore the same c_0 and c_1 were used for all values of F. For a very weak force ($F = 0.1$, not shown), the controllers have similar performance. As the strength of the force increases ($F = 0.3$ to $F = 0.53$) the nonlinear controller consistently performs well. Conversely, performance of the linearization based controller begins to degrade as the overestimating nature of the gain induces oscillation and the origin transitions from stable, to marginally stable, to unstable. For a strong force ($F = 2$) the nonlinear controller is still able to stabilize the origin. The gain scheduled controller extends the range of stability to $F = 2.8$ (not shown), which is the largest value for which the nonlinear controller (with $c_0 = 10$) preserves stability of the origin. Simulations with $F = 2.8$ show that increasing the value of c_0 improves performance, suggesting that c_0 should be increased proportional to F, though ultimately the gain scheduling based nonlinear controller cannot stabilize the origin for very large F. The simulations
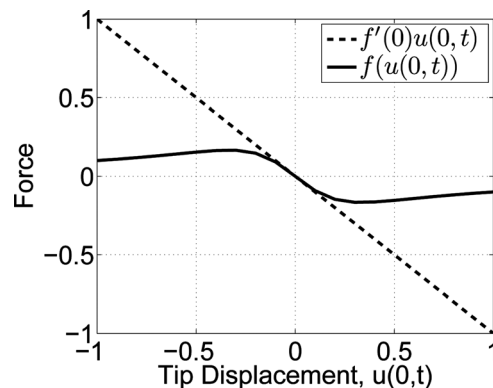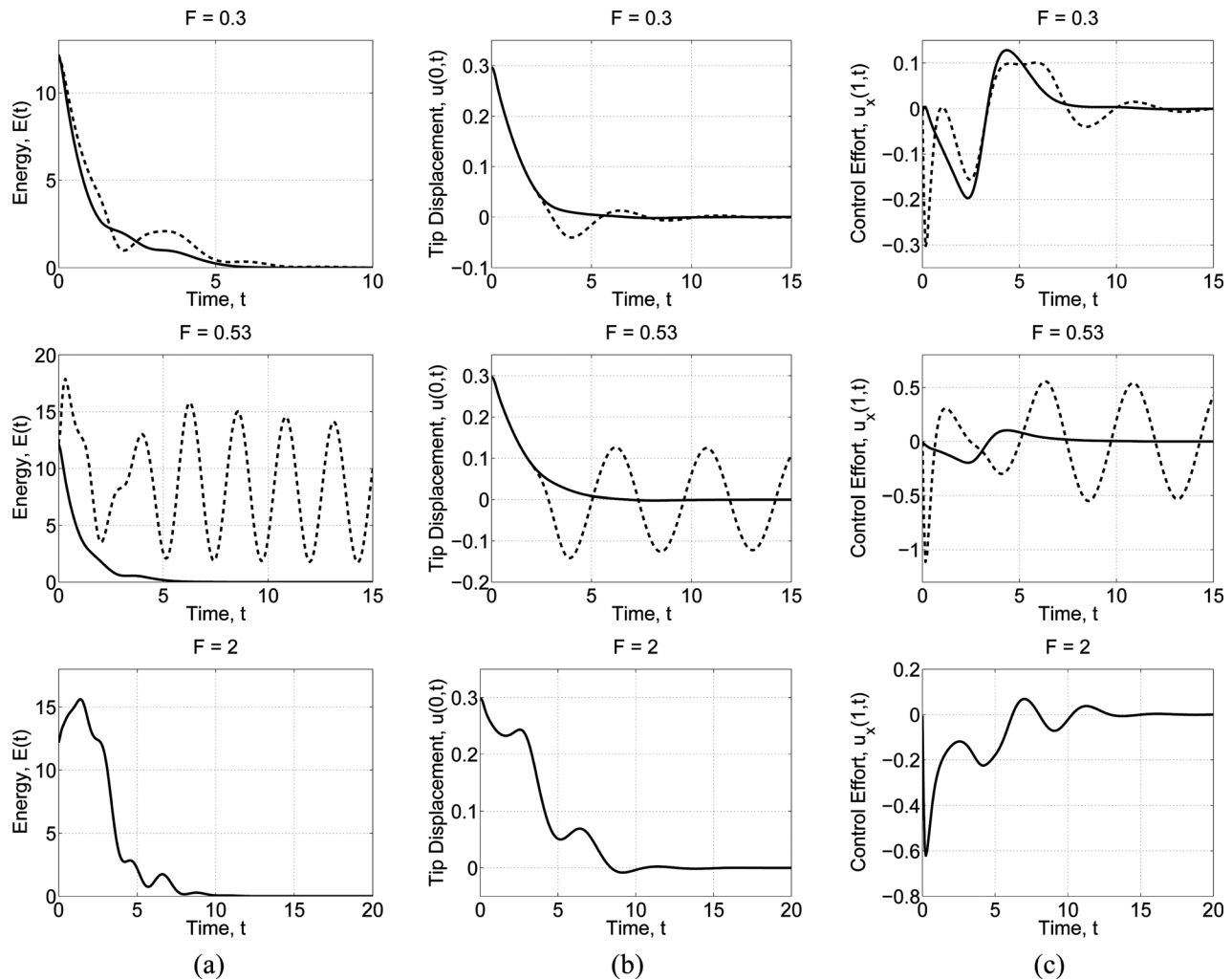

Fig. 4 Comparison of the nonlinearity $f(u(0,t))$ used for the beam simulations, and its linear approximation $f'(0)u(0,t)$, for $F = 1$.

Fig. 5 Beam simulation results showing the closed-loop system with linearization based control (dashed) and gain scheduling based nonlinear control (solid). The beam is initialized with $u_0(x) = \frac{3}{10}(1-x)^2$ and $\alpha_0(x) = -\frac{3}{5}(1-x)$ and zero velocities, and the nonlinearity strength is varied as $F = \{0.3, 0.53, 2\}$. The plots compare the (a) energy $E(t)$, (b) tip displacement $u(0,t)$, and (c) boundary control effort $u_x(1,t)$.

show that—for a nonlinearity where the linearization overestimates the force—the nonlinear controller outperforms the linearization based controller when the nonlinear interaction force becomes sufficiently strong, and it extends the range of stability.

Figure 6 compares the performance of the linearization based controller and gain scheduling based nonlinear controller when the goal is to generate and track the reference trajectory $u^r(0,t) = 0.5\sin(\pi t/3)$, $\alpha^r(0,t) = 0$. The beam is initialized with zero initial conditions. The plot shows how the linearization based controller begins to generate the reference trajectory, but in overestimating the nonlinearity it applies an excess of control effort producing large amplitude and phase errors, and cannot compensate for the harmonics caused by interaction with the nonlinearity. The linearization based controller eventually destabilizes the system for larger time. The gain scheduling based nonlinear controller is able to generate and track the sinusoid with very small errors in amplitude and phase, part of which can be attributed to the approximate nature of the shear beam results applied to the Timoshenko beam [29,30]. The controllers have comparable performance for small reference amplitudes and force strengths, the gain scheduled controller outperforms the linearization based controller when the reference amplitude or force strength increases, and neither controller can stabilize the reference trajectory when the strength of the force is too large.
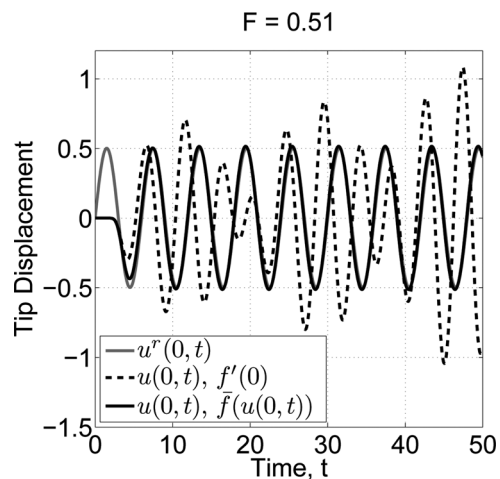
Fig. 6 Beam simulation results comparing the tip displacement and reference trajectory when boundary control is applied with linearization based control and gain scheduling based nonlinear control.

7 Conclusions

A control design for nonlinear PDEs inspired by gain scheduling and based on the backstepping theory for linear PDEs has been introduced. Control designs were presented for a benchmark first-order hyperbolic PDE with boundary-value-dependent in-domain nonlinearity, and for the string and shear beam with Kelvin–Voigt damping and boundary-displacement-dependent free-end nonlinearities. The benchmark system was used to illustrate how one can perform a stability analysis of a nonlinear PDE system with gain scheduling based nonlinear control. Stability analysis showed that the equilibrium $u \equiv 0$ of the closed-loop system was locally exponentially stable. String and Timoshenko beam simulations were presented to show the performance of the gain scheduling based nonlinear controllers, which outperformed simple linearization based controllers.

Gain scheduling based PDE boundary backstepping methods provide a simple and effective solution to the difficult problem of nonlinear control design for infinite dimensional nonlinear systems. While not as powerful as a full nonlinear design, gain scheduling based PDE backstepping theory produces tractable results that outperform simple linearization based design.

Acknowledgment

References

[1] Boskovic, D., and Krstic, M., 2001, "Nonlinear Stabilization of a Thermal Convection Loop by State Feedback," Automatica, **37**, pp. 2033–2040.
[2] Boskovic, D., and Krstic, M., 2002, "Backstepping Control of Chemical Tubular Reactors," Comput. Chem. Eng., **26**, pp. 1077–1085.
[3] Boskovic, D., and Krstic, M., 2003, "Stabilization of a Solid Propellant Rocket Instability by State Feedback," Int. J. Robust Nonlinear Control, **13**, pp. 483–495.
[4] Armaou, A., and Christofides, P. D., 2000, "Wave Suppression by Nonlinear Finite-Dimensional Control," Comput. Chem. Eng., **55**(14), pp. 2627–2640.
[5] Armaou, A., 2004, "Output Feedback Control of Dissipative Distributed Processes Via Microscopic Simulations," Comput. Chem. Eng., **29**(4), pp. 771–782.
[6] Varshney, A., Pitchaiah, S., and Armaou, A., 2009, "Feedback Control of Dissipative PDE Systems Using Adaptive Model Reduction," AIChE J., **55**(4), pp. 906–918.
[7] Christofides, P. D., 2001, *Nonlinear and Robust Control of PDE Systems: Methods and Applications to Transport-Reaction Processes*, Birkhäuser, Boston, MA.
[8] Kugi, A., Thull, D., and Kuhnen, K., 2006, "An Infinite-Dimensional Control Concept for Piezoelectric Structures With Complex Hysteresis," Struct. Control Health Monit., **13**, pp. 1099–1119.
[9] Meurer, T., and Zeitz, M., 2005, "Feedforward and Feedback Tracking Control of Nonlinear Diffusion-Convection-Reaction Systems Using Summability Methods," Ind. Eng. Chem. Res., **44**, pp. 2532–2548.
[10] Banach, A. S., and Baumann, W. T., 1990, "Gain-Scheduled Control of Nonlinear Partial Differential Equations," *Proceedings of the Conference on Decision and Control*, pp. 387–392.
[11] Vazquez, R., and Krstic, M., 2008, "Control of 1-D Parabolic PDEs With Volterra Nonlinearities—Part I: Design," Automatica, **44**, pp. 2778–2790.
[12] Vazquez, R., and Krstic, M., 2008, "Control of 1-D Parabolic PDEs With Volterra Nonlinearities—Part II: Analysis," Automatica, **44**, pp. 2791–2803.
[13] Cloutier, J. R., 1997, "State-Depedent Riccati Equation Techniques: An Overview," *Proceedings of the American Control Conference*, pp. 932–936.
[14] Cloutier, J. R., and Stansbery, D. T., 1999, "Control of a Continuously Stirred Tank Reactor Using an Asymmetric Solution of the State-Dependent Riccati equation," *Proceedings of the IEEE International Conference on Control Applications*, pp. 893–898.
[15] Cloutier, J. R., and Stansbery, D. T., 2002, "The Capabilities and Art of State-Dependent Riccati Equation-Based Design," *Proceedings of the American Control Conference*, pp. 86–91.
[16] Khalil, H. K., 2002, *Nonlinear Systems*, 3rd ed., Prentice Hall, Upper Saddle River, NJ.
[17] Rugh, W. J., 1990, "Analytical Framework for Gain Scheduling," *Proceedings of the American Control Conference*, pp. 79–84.
[18] Rugh, W. J., and Shamma, J. S., 2000, "Research on Gain Scheduling," Automatica, **36**, pp. 1401–1425.
[19] Shamma, J. S., and Athans, M., 1990, "Analysis of Gain Scheduled Control for Nonlinear Plants," IEEE Trans. Autom. Control, **35**(8), pp. 898–907.
[20] Shamma, J. S., and Athans, M., 1991. "Gain Scheduling: Potential Hazards and Possible Remedies," *Proceedings of the American Control Conference*, pp. 101–107.
[21] Shamma, J. S., and Athans, M., 1991, "Guaranteed Properties of Gain Scheduled Control for Linear Parameter-Varying Plants," Automatica, **27**(3), pp. 559–564.
[22] Shamma, J. S., and Cloutier, J. R., 2003, "Existence of SDRE Stabilizing Feedback," IEEE Trans. Autom. Control, **48**, pp. 513–517.
[23] Wang, J., and Rugh, W. J., 1987, "Feedback Linearization Families for Nonlinear Systems," IEEE Trans. Autom. Control, **32**(10), pp. 935–940.
[24] Wang, J., and Rugh, W.J., 1987, "Parameterized Linear Systems and Linearization Families for Nonlinear Systems," IEEE Trans. Circuits Syst., **34**(6), pp. 650–657.
[25] Krstic, M., and Smyshlyaev, A., 2008, *Boundary Control of PDEs: A Course on Backstepping Designs*, SIAM, Philadelphia, PA.
[26] Krstic, M., and Smyshlyaev, A., 2008, "Backstepping Boundary Control for First-Order Hyperbolic PDEs and Application to Systems With Actuator and Sensor Delays," Syst. Control Lett., **57**, pp. 750–758.
[27] Krstic, M., Guo, B.-Z., Balogh, A., and Smyshlyaev, A., 2008, "Output-Feedback Stabilization of an Unstable Wave Equation," Automatica, **44**, pp. 63–74.
[28] Krstic, M., Siranosian, A. A., Balogh, A., and Guo, B.-Z., 2007, "Control of Strings and Flexible Beams by Backstepping Boundary Control," *Proceedings of the American Control Conference*.
[29] Siranosian, A. A., Krstic, M., Smyshlyaev, A., and Bement, M., 2008, "Motion Planning and Tracking for Tip displacement and Deflection Angle for Flexible Beams," *Proceedings of the American Control Conference*.
[30] Siranosian, A. A., Krstic, M., Smyshlyaev, A., and Bement, M., 2009, "Motion Planning and Tracking for Tip Displacement and Deflection Angle for Flexible Beams," ASME J. Dyn.Syst., Meas., Control, **131**, p. 031009.
[31] Krstic, M., Guo, B.-Z., Balogh, A., and Smyshlyaev, A., 2008, "Control of a Tip-Force Destabilized Shear Beam by Observer-Based Boundary Feedback," SIAM J. Control Optim., **47**, pp. 553–574.
[32] Krstic,M., and Balogh, A., 2006, "Backstepping Boundary Controller and Observer for the Undamped Shear Beam," *17th International Symposium on Mathematical Theory of Networks and Systems*.
[33] Krstic, M., Siranosian, A. A., and Smyshlyaev, A., 2006, "Backstepping Boundary Controllers and Observers for the Slender Timoshenko beam: Part I—Design," *Proceedings of the American Control Conference*.
[34] Krstic, M., Siranosian, A. A., Smyshlyaev, A., and Bement, M., 2006, "Backstepping Boundary Controllers and Observers for the Slender Timoshenko beam: Part II—Stability and Simulations," *Proceedings of the IEEE Conference on Decision and Control*.
[35] Han, S. M., Benaroya, H., and Wei, T., 1999, "Dynamics of Transversely Vibrating Beams using four engineering theories," J. Sound Vib., **225**, pp. 935–988.
[36] Zhao, H. L., Liu, K. S., and Zhang, C. G., 2004, "Stability for the Timoshenko Beam System With Local Kelvin–Voigt damping," Acta Math. Sin. English Ser., **21**(3), pp. 655–666.